Ab initio modeling of primary processes in photosynthesis : protein induced activation of bacteriochlorophylls for efficient light harvesting and charge separation

Wawrzyniak, P.K.

Chapter 1

Introduction

1.1 Photosynthesis

Photosynthesis on Earth can be traced 3.5 billion years back in time when algae species developed a photosynthetic apparatus similar to present plant photosystems. [2, 3] Since then, all the food, oxygen for respiration and energy produced through the molecular respiration, are directly or indirectly related to the photosynthetic activities. It is believed that phototrophic organisms converted the composition of Earth's atmosphere over the history of our planet from the anoxic state to the oxic state by production of oxygen. However, only plants, algae and cyanobacteria are capable of performing oxygenic photosynthesis. [4] The other types of photosynthetic bacteria, *i.e.* purple sulphur bacteria, purple non-sulphur bacteria, green sulphur bacteria, green non-sulphur bacteria and heliobacteria, are not able to oxidize water and thus do not produce oxygen. [5] Instead, they use reduced sulphur compounds, molecular hydrogen or simple organic molecules as an electron donor to obtain reductive power. There are two essential steps in photosynthesis: absorption of light and conversion of excitation energy into chemical energy for convenient energy storage. The course of events in photosynthesis starts with an absorption of a photon by one of the pigment molecules in the photosynthetic membrane. Then the excitation is transferred through an array of antenna pigments, otherwise known as light-harvesting complexes,

to the reaction center, which acts as a photochemical trap to convert the excitations into chemical energy. Before the components of the photosynthetic apparatus will be discussed in more details, an overview of histidine protonation states will be presented, as this aminoacid occupies crucial positions in photosynthetic complexes.

1.2 Histidine

Histidine is one of the 20 naturally occurring amino acids and plays an important role in many biochemical processes. Histidine can act as a catalyst in the active site of enzymes [6] and as a ligand to metals. [7–12] It can undergo tautomeric changes and is able to form hydrogen bonds, acting both as a proton donor and acceptor, and thus playing the role of a mediator in proton transfer processes in various proteins. [13, 14] Four different protonation forms of the imidazole ring are possible: a formally anionic imidazolate form, denoted as anionic in this thesis, two neutral tautomers and a doubly protonated imidazolium form, named cationic here. The neutral tautomers will be denoted throughout this dissertation as neutral$_\pi$ and neutral$_\tau$, with N_π or N_τ protonated respectively (see Figure 1.1). In the literature N_π is sometimes

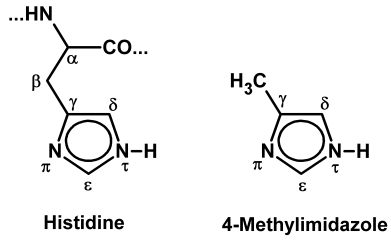

Figure 1.1: The neutral$_\tau$ form of histidine and 4-methylimidazole with the atom labeling used throughout the thesis.

referred to as N^δ or N_3 and N_τ is indicated as N^ε or N_1. The neutral$_\tau$ histidine is the most frequently found in nature, especially in proteins and smaller compounds. [15–20] The other neutral tautomer is difficult to crystallize and we are aware of only one crystalline sample of glutaric acid–histidine complex where it has been observed. [21] Moreover, it is only occasionally found

in proteins where it is stabilized by a hydrogen bond and is believed to be reserved for special tasks. [22–24] These two tautomers can be distinguished in a NMR spectrum by their C_δ chemical shifts. [25] Specifically, values of C_δ chemical shift above 122 ppm were assigned to the neutral$_\pi$ tautomer, while values below 122 ppm indicate the presence of the neutral$_\tau$. The two nitrogens in the neutral tautomers have substantially different character. The pyrrole-type nitrogen, denoted often as >N–H, gives experimentally a NMR resonance at 170 ppm and its chemical shift anisotropy in histidine is estimated to be $\delta \approx 4.5$ kHz with $\eta \approx 1$. [18, 26, 27] In contrast, the pyridine-type nitrogen, denoted usually as $\geqslant$N|, gives a NMR signal around 250 ppm, with anisotropy parameters δ and η of about 8.7 kHz and 0.4, respectively. [18, 26, 27]

The existence of the two neutral tautomeric forms is described by the equilibrium constant, which for different imidazoles depends on the nature of the ring substituent group [28] and equals 1 for imidazole itself. Since for the imidazole (no ring substituents) both nitrogen atoms are chemically equivalent and the tautomeric exchange is fast in aqueous solution, only one average signal is observed for ^{15}N NMR [23], while two resonances separated by 72 ppm are reported for polycrystalline imidazole, suggesting that the tautomeric exchange is very slow or not existing in a crystal phase. [29] The NMR signal in solution is observed to shift upfield with decreasing pH, producing a smooth titrating curve and thus indicating that the ionic equilibrium is also fast on the NMR time scale.

For histidine in solution, due to the presence of α-amino group ionization and due to the fact that the ring nitrogens are not equivalent, the situation is more complex. Therefore, five possible species must be considered, as depicted in Fig. 1.2. At low pH only the positively charged form I is present and the π and τ nitrogens give signals separated by 2.4 ppm. [30] With increasing the pH a deprotonation of the imidazole ring of histidine occurs and the neutral forms IIa and IIb are produced, but until pH 8.0 is reached all the three species yield an averaged ^{15}N chemical shift due to rapid chemical exchange. At pH 8.0 the cationic form is not present anymore. At this point, the N_π signal is shifted downfield by 56 ppm when compared to the positively charged histidine, while N_τ is shifted only by 5 ppm, indicating that the de-

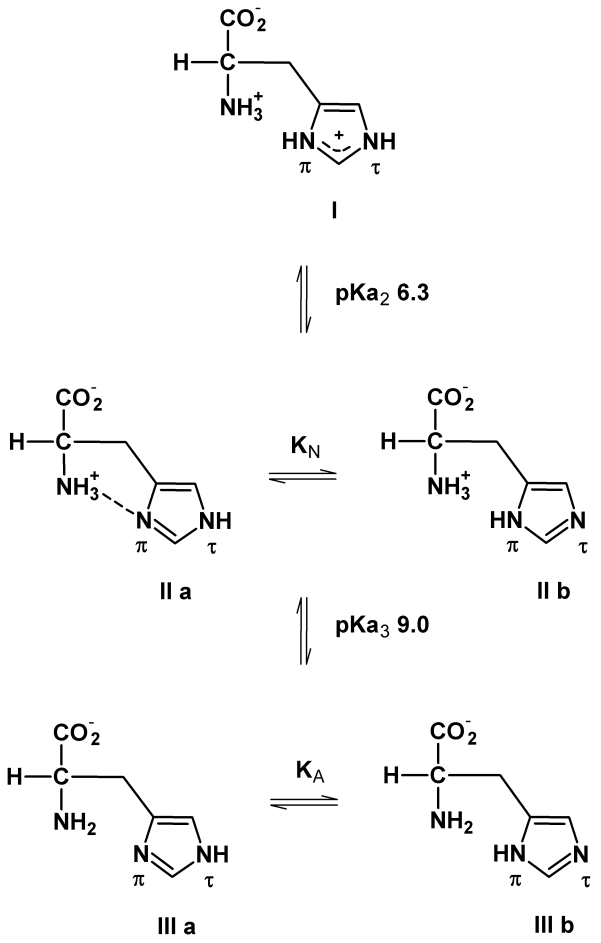

Figure 1.2: Possible ionic and tautomeric forms of histidine from pH 2 to 12.5. Redrawn from [29].

protonation occurs mainly at the π position. To support this observation, the molar fraction of IIa was estimated, resulting in a value of 0.88, and thus confirming that this tautomer exists in a predominant quantity. Nevertheless, a significant amount of the other tautomer is present, giving rise to average ^{15}N chemical shift values. The reason that the IIa form is predominant may be, at least partially, attributed to a hydrogen bond between unprotonated N_π and the α-amino group, which cannot be formed in the tautomer IIb due to steric hindrance. [31] Further deprotonation, occurring at the amino group, removes the possibility for hydrogen bond formation, resulting in a redistribution of the tautomers: the N_π peak shifts upfield by 15 ppm and the N_τ peak shifts downfield by the same amount. Now the IIIa form is not so strongly favored over IIIb as for the neutral form, however the calculated molar fraction (0.76) indicates that the tautomer with the proton attached to N_τ is still the predominant one.

According to solid-state studies [29], in samples lyophilized at low pH, the N_π and N_τ signals are very close to the corresponding cationic chemical shifts in solution. When the pH increases to 8.4 the positively charged histidine is replaced by a neutral one, however, contrary to the liquid studies a separate resonance for each species is observed because the exchange between the cationic and neutral forms is very slow. In addition, only the neutral$_\tau$ tautomer is present, as revealed by 11 ppm downfield shift compared to the N_π response in solution and 5 ppm upfield shift of the N_τ signal. The midpoint for that transition was calculated to occur at pH 6.3. Further increase of the pH leads to a negatively charged form and the conversion is complete at pH 12.3. The midpoint of this transition occurs around pH 9.5 and the deprotonation results in a 6 ppm downfield shift of the π resonance with little change of the τ frequency. This is an evidence that the neutral$_\tau$ tautomer is still the only one observed, even though the stabilization provided by the hydrogen bond in the neutral form is now absent due to the deprotonation of the α-amino group.

Since histidine activity depends on the nitrogen atoms in the imidazole ring, many biochemical mechanisms may be understood only if histidine protonation states can be established. However, many histidine protonation states

reported in Protein Data Bank structures are still tentative. [32] In principle such information can be obtained from NMR studies. [22, 25, 33–35] The problem is that even if NMR spectra are available, a precise assignment of the spectral lines to a specific residue is often difficult. Quantum chemical calculations can then provide a complementary tool to assist in assigning the NMR spectra.

1.3 The Light-Harvesting Complex II of *Rhodopseudomonas acidophila*

Light-harvesting complexes absorb photons and transport the excitation energy through LH1 complexes to photosynthetic reaction centers, where a series of electron transfer reactions across the membrane leads to charge separation. In this way, LH2 complexes accomplish the first step of photosynthesis, *i.e.* the absorption of light. The optical absorption happens much faster and over a much larger area, compared to the charge separation in the RC, which is a relatively slow and local process. The structure of LH2 from *Rhodopseudomonas acidophila* has been described in detail before. [36–38] Experimentally [36], it has been found that this antenna system possesses a 9-fold symmetry, as depicted in Fig. 1.3. It contains a ring of 9 bacteriochlorophyll *a* molecules constituting the B800 system, named after its characteristic absorption at 800 nm. In addition another 18 BChl *a* molecules are arranged in pairs of α and β molecules with partial macrocycle overlap, which form the B850 ring system. The planes of the B800 macrocycles are aligned parallel to the membrane, while the macrocycle planes of the BChls *a* in the B850 ring are perpendicular to the membrane. [36] The distance between two Mg atoms in B800 is 20.8–21.1 Å, while it is 9.2–9.4 Å within an (α,β)-B850 dimer and 8.8–9.0 Å between two following B850 dimers.

In the LH2 complex, helical protein subunits form two concentric cylinders, an inner ring of α-protein subunits and an outer ring of β-protein subunits. An α-subunit monomer consists of 53 residues and the β-subunit monomer consists of 41 residues. The magnesium atoms of each B850 (α,β)-BChl *a* dimer ligate N_τ atoms from α-His 31 or β-His 30 residues, respec-

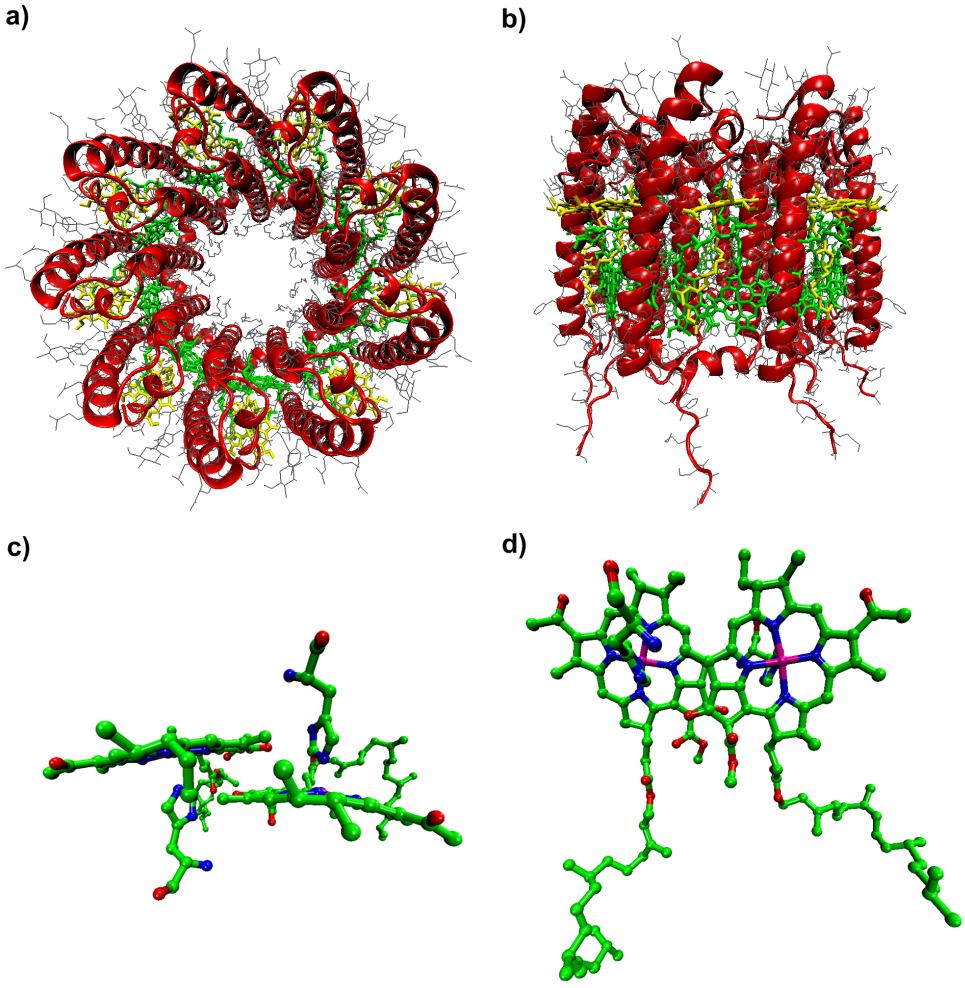

Figure 1.3: a) Top view and b) side view of LH2 complex from the 2FKW crystal structure of *Rps. acidophila*. [36] The B850 and B800 BChl *a* are shown in green and in yellow, respectively. c) Top view and d) side view of a B850 dimer and coordinated histidines.

tively. [26, 39] The α and β histidines alternate when moving along the ring of B850. Three other histidines, α-His 37, β-His 12 and β-His 41, are not coordinated to BChls. A complete assignment of the histidine residues in the LH2 complex of *Rps. acidophila* has been recently obtained by solid-state NMR. [26, 39] It was found that the five histidines in the LH2 complex can be classified in two types. The first type, including α-His 37 and β-His 12, has chemical shifts corresponding to neutral$_\tau$ histidines, while the α-His 31, β-His 30 and β-His 41 have been classified as positively charged histidines and all three display identical ^{13}C chemical shifts. [26, 39] However, while the β-His 41 has both nitrogens in the ring protonated, the α-His 31 and β-His 30 are coordinated by the N_τ nitrogen to the Mg^{2+} ion of the bacteriochlorophyll *a* molecules. Therefore, the residues α-His 31 and β-His 30 are formally neutral$_\pi$ tautomers, which is consistent with the experimentally measured anisotropy parameters for N_τ, indicating a pyridine-like chemical character of this atom. [26, 39] Other metal-coordinated histidines maintain their neutral character and show chemical shifts similar to the uncoordinated neutral histidines. [40] Thus, the experimental observation of ^{13}C chemical shifts for the Mg-coordinated histidines that are very similar to the shifts for the cationic β-His 41 [26, 39] is surprising and in contrast with the anisotropy parameters δ and η.

The two BChl *a*-coordinated histidines stabilize the B850 ring assembly and mediate the coupling between the ring components, playing not only structurally but also electronically an important role. [41] The ring itself acts, through the overlapping assembly, as an energy storage system that preserves excitation energy until it is forwarded to other rings and ultimately to the RC. [42, 43] For the B800, the excitations are localized on one BChl *a* before jumping to the next one, while the B850 system is strongly exciton-coupled and excitations are effectively delocalized over the entire B850 ring. [44, 45] Since, the exact mechanism of the energy storage and the color shift is not yet fully elucidated, knowledge of the electronic structure of the BChl *a*–His complex can be important for understanding the exciton transfer process over the LH2 B850 ring.

1.4 Bacterial Reaction Center of *Rhodobacter sphaeroides*

The primary photosynthetic energy conversion occurs in pigment–protein complexes known as reaction centers. Two types of RCs are known. [46, 47] Type-I possesses iron–sulphur clusters as terminal electron acceptors, while in type-II this function is performed by quinones. All the anoxygenic photosynthetic organisms contain either type-I RCs, in green sulphur bacteria and heliobacteria, or type-II RCs in purple bacteria and green non-sulphur bacteria. In contrast, in oxygenic organisms both types are present and work in series: the type-I RC or Photosystem I reduces carbon dioxide via the Calvin cycle, while the type-II RC, Photosystem II, is involved in oxidization of water.

The reaction center of *Rb. sphaeroides*, belonging to the class of type-II RCs, is surrounded by light-harvesting complexes LH1 and LH2. Together they form the photosynthetic unit located in vesicles of the cytoplasmic membrane. The RCs consist of three single polypeptide chains, forming L, M and H subunits. [48–50] The first two subunits consist of 281 and 307 aminoacids, respectively. They exhibit mainly α-helical structure and both have five long hydrophobic α-helices that span the bacterial membrane. The H chain, formed by 260 residues, is more globular in shape and is almost entirely positioned in the cytoplasmic region with only one transmembrane helix. Apart from the three polypeptide chains, ten non-covalently bound prosthetic groups, usually referred to as cofactors, are present: Four bacteriochlorophylls *a*, two bacteriopheophytins *a* and two ubiquinones-10 form two branches **A** and **B** with a non-heme iron ion (Fe^{2+}) in between, while the tenth cofactor, the carotenoid spheroidene, is located on the side of branch **B** (Fig. 1.4). The structures of cofactors directly involved in the electron transfer are presented in Fig. 1.5.

Two of the four bacteriochlorophylls *a* (P_L from the **A** branch and P_M from the **B** branch) have mutual overlap with their pyrrole ring *I* (see Fig. 1.5) with a minimum intermolecular distance of approximately 3.3 Å, and they connect the two cofactor branches. [50] Since they are electronically coupled and the primary electron transfer originates from these two species, they are

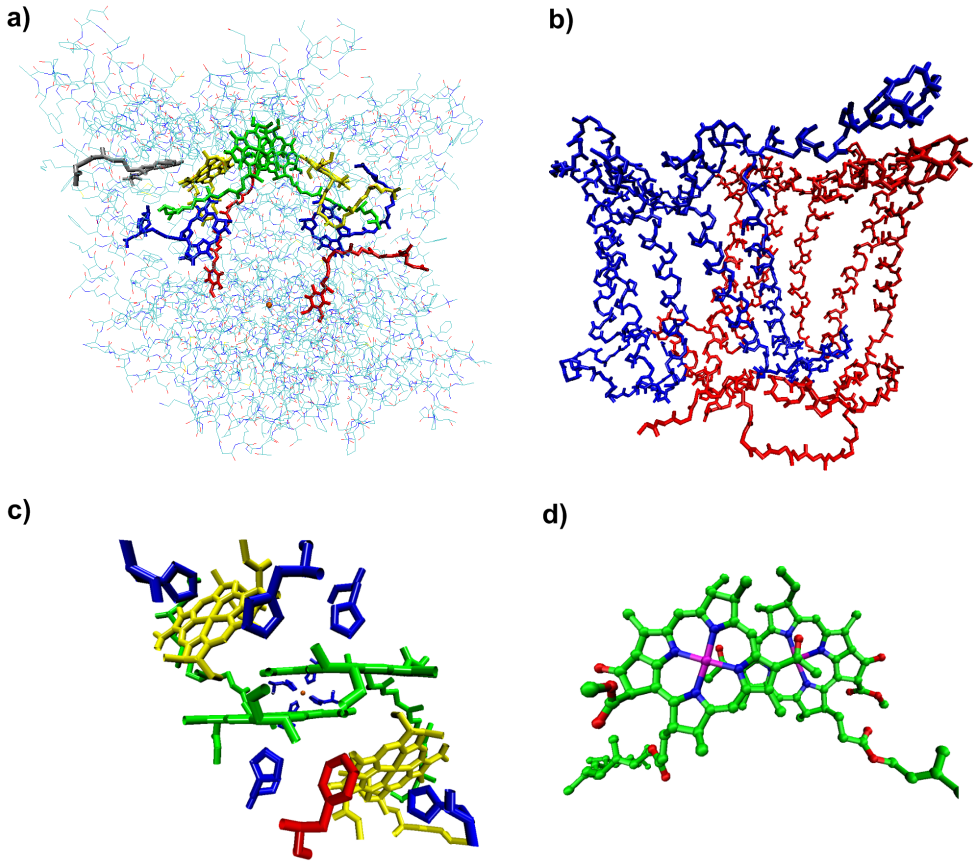

Figure 1.4: a) Structure of the bacterial reaction center and arrangement of cofactors in the 1PCR crystal structure of *Rb. sphaeroides* [49]: *P* (green), *B* (yellow), φ (blue), *Q* (red), *Fe* (orange) and *C* (grey). The active branch is on the right side. b) Symmetry of L (blue) and M (red) protein backbones. c) Overview of the special pair: P (green), histidines (blue) and phenylalanine (red). d) Structure and overlap of the special pair.

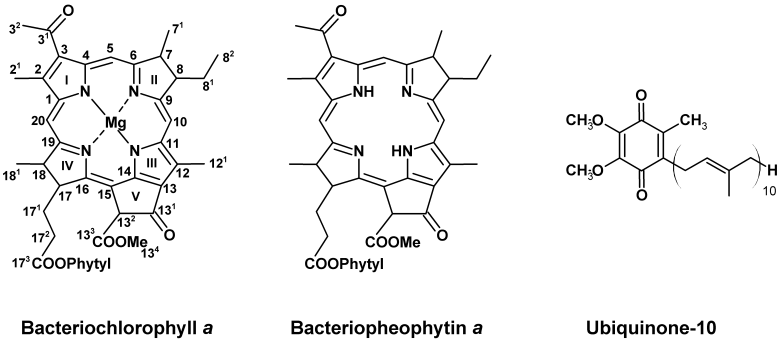

Figure 1.5: Structure of cofactors directly involved in electron transfer. The left panel shows the IUPAC numbering of carbon atoms for the BChl *a* which is used throughout the thesis.

usually called the 'Special Pair'. A monomeric accessory BChl *a* molecule is located on either side of the special pair and two bacteriopheophytin *a* species reside about 18 Å away from P (Fig. 1.4). The magnesium atoms of P_L and P_M ligate His L173 and His M202, respectively. Two other histidine residues, His L153 and His M182, coordinate to the two accessory bacteriochlorophylls *a*. These histidines are within about the same distance (2.68 ± 0.07 Å) from the corresponding BChl *a* and should experience similar ring current shifts. The ring current shift is a change of the nuclear resonance frequency due to the field-induced circulation of delocalized π electrons in proximity. Interestingly, the two histidines interacting with the special pair are within hydrogen-bonding distance to a water molecule with their N_π atoms. [50] In addition, His L168 is located at hydrogen-bonding distance from the acetyl bonded to the P_L C3 atom, while the symmetrical position for the P_M is occupied by Phe M197. Contrary to LH2, protonation states of these and remaining histidines of the BRC have not yet been clearly established.

The two cofactor branches, together with polypeptide backbones of protein subunits L and M, display a nearly perfect local two-fold symmetry (Fig. 1.4), with the symmetry axis oriented perpendicular to the membrane plane. [2] Also the overlap of the special pair appears to be rather symmetric. Despite this structural symmetry, the functioning of the reaction center is asymmet-

ric and in the wild type bacteria electron transfer takes place through the "active branch" **A**. [51] It is not known if and how the protein initiates the charge transfer across the active branch. In the primary electron transfer event, the special pair is excited by the energy transferred from the light-harvesting complexes. Within 3 ps an electron is transferred from the first excited singlet state of P to φ_A forming the radical pair $P^{+\bullet}\varphi_A^{-\bullet}$. [2,52] There is converging and convincing evidence that the accessory B_A is an intermediate of this process. [2,3,53–57] In the next step, the electron is transferred down a chain of acceptor molecules to Q_A and subsequently to Q_B of the **B** branch, reducing it once. These secondary electron transfers are considerably slower, with reported kinetics of 200 ps and 100 μs for the two steps, respectively. [3] As a consequence of those primary and secondary electron transfers, a long-lived, spatially well-separated radical pair is formed. Meanwhile, after about 1 μs, the oxidized primary electron donor $P^{+\bullet}$ is reduced by an electron from cytochrome c located at the periplasmic side of the protein. It takes an additional electron and two protons to create ubiquinol QH_2, which leaves the RC and is replaced by ubiquinone-10 from the quinone pool in the organism. [58] QH_2 is used to facilitate the creation of a proton gradient across the membrane that drives the synthesis of the energy-rich ATP. [59]

This strong contrast between symmetry in structure and asymmetry in function has triggered investigations in the direction of electron transfer for many years [2,3] and a considerable amount of studies have focused on the special pair. [53,60–66] It has been proposed from Stark experiments that the excited state P* is electronically asymmetric and more electron density is concentrated on P_M. [63] For the cation radical $P^{+\bullet}$, EPR and ENDOR studies have shown a disproportion in spin density distribution in favor of P_L. [64,67,68] It has been also reported that the two bacteriochlorophylls *a* of the special pair have different electronic structure already in the ground state and that excess negative charge is located on P_L. [53,65,66,69–71] Therefore, the functional asymmetry in the RC is introduced in the dark ground state, although the origin of the symmetry breaking remains unclear.

1.5 Scope of the Thesis

Although the structure and the kinetics of the electron transfer in bacterial reaction centers are known, how the functional asymmetry in this protein triggers the charge separation may be considered one of the central questions for the conversion of solar energy into chemical energy in photosynthetic organisms. With a detailed understanding of the origin for the special pair symmetry breaking and its influence on the electron transfer, it would be possible to gain an insight into the generic mechanism underpinning the principles of an efficient charge separation process. This may prove beneficial for the development of artificial photosynthetic devices, which would not only offer a great potential for solving the global energy problem but also would assist in mitigating climate change.

Specifically, the immediate protein environment of the special pair, particularly histidine residues, may perturb the electronic structure of P_L and P_M in the ground and excited states, facilitating thereby the electron transfer along the **A** branch. Since histidine activity depends on the nitrogen atoms in the imidazole ring, it is crucial to know the protonation states of the imidazole side chains. However, presently no detailed knowledge of histidine protonation states in bacterial reaction centers exists and X-ray crystallography cannot provide a clear answer about the specific protonation state of residues such as His. [32] NMR, combined with quantum mechanical calculations, provides a complementary method in structure determination and structure-function studies for the histidines.

As discussed in the previous sections, Mg-coordinated histidines in the LH2 complex are not only structurally but also electronically important for stabilization and coupling between the B850 bacteriochlorophylls *a*. Therefore, a detailed knowledge of the electronic structure of the BChl *a*–His complex is essential to understand the exact mechanism of energy storage and exciton transfer over the B850 ring. Recent experimental data reveal a rather unusual behavior for those histidines. [26,39] Despite their formal neutral$_\pi$ form, they surprisingly exhibit chemical shifts identical to the doubly protonated histidines. This issue can be addressed only by means of quantum mechanical calculations.

The specific aim of this thesis is to investigate interactions between histidine and bacteriochlorophylls *a* in LH2 and BRC systems, and address the open questions posed by experimental data as to the nature of BChl *a*–His complexes and asymmetry of special pair. The theoretical work presented here describes the study of photosynthetic processes in purple non-sulphur bacteria *Rhodobacter sphaeroides* and *Rhodopseudomonas acidophila* and is closely related to recent experimental work in the field of photosynthesis.

In chapter **2**, a general overview of theoretical methods and approximations used in this work is presented. Chapter **3** describes accuracy assessments for DFT-computed chemical shifts and presents the chemical shift characterization of neutral$_\pi$ histidine, for which a very limited set of data exists. Next, protonation states of uncoordinated histidines are discussed, and finally the BChl *a*–His complex in the LH2 protein is addressed with its peculiar properties. It is established that Mg-coordinated histidines are in a protein-induced frustrated state due to steric and electrostatic stress exerted by the LH2 protein environment. In chapter **4** an assignment of histidine protonation states in the reaction center is presented, both for axial and non-axial histidines. It is found that one of the four Mg-coordinated histidines has a substantially different electronic structure compared to the other three, possibly contributing to the differences between P_L and P_M in the ground and excited state. A more detailed discussion on asymmetry of the special pair is presented in chapter **5**, where an extended model including explicitly the special pair and the closest residues is studied with DFT. It is proposed that the asymmetry of the special pair is an intrinsic property of the bacteriochlorophyll *a* dimer resulting from a particular orientation of the P_L 3^1 acetyl group. This orientation is forced by the hydrogen bond from His L168 and by inducing conformational changes to the acetyl the biophysical properties of the special pair can be tuned. Finally, chapter **6** provides a general discussion and presents some future prospects.